FPGA and MATLAB Based Solution for Retinal Exudate Detection

Vasanthi Satyananda, Narayanaswamy K. V., Karibasappa

Abstract: Now-a-days, image processing is extensively used for analysis of several biomedical images to identify the complications in one's health. Most of the solutions offered are based on application software. Since these solutions are expensive, an embedded system approach is being explored in the recent years, considering its cost-effectiveness. This paper propounds an embedded system approach to identify exudates in retinal images. These exudates are often identified as indicators of a medical disorder known as Diabetic Retinopathy, which is one of the medical complications that arise due to high blood sugar levels. The algorithm employs statistical analysis using histogram to enhance the contrast of the images, thus assisting in extracting exudates by utilising the elementary concepts of image processing. Since the pixel characteristics of exudates and optic disk match, it becomes inevitable to first eliminate optic disk from retinal images, and then extract exudates. The prototype has been developed on MATLAB and is downloaded on an Artix 7 FPGA with minimal usage of its resources. The system proposed in this paper results in an accuracy of 90%.

Keywords: Diabetic Retinopathy, Exudates, FPGA, Image Processing, Histogram, Labeling, Optic Disc, Elimination, MATLAB.

I. INTRODUCTION

Healthcare Engineering is defined as "the involvement of aspects of engineering to assist in diagnosis, treatment and prevention of illness" [1]. This discipline covers development of basic instruments used in biological fields like stethoscope and thermometer, to complex machines like X-Ray Machines, Magnetic Resonance Image Scanners and scalpel-wielding robots to automated diagnosis machines such as Automated DNA Sequencer and Blood Chemistry Analyzer. Along with inventing and implementing above mentioned systems, this field also encompasses development of algorithms to detect disorders such as cancer [2], brain tumor [3], skin diseases [4]

and many more. The algorithms often are implemented as a "software package" which utilizes general-purpose processors. Though these devices offer workability of varying any parameters concerned with the algorithm at any time, inefficacy related to the speed and resource allocation stay unresolved. On the other hand, implementing an algorithm entirely on hardware may resolve the above-mentioned issues, but are not feasible when it comes to processing images of higher dimensions. Thus, as a solution, a combination of both hardware and software, known as an "embedded system" is preferred which can harness the advantages of both platforms [5].

The condition where blood sugar level varies either above or below normal threshold is called Diabetes Mellitus [6]. One of the disorders associated with Diabetes is Diabetic Retinopathy (abbreviated as DR). DR summarizes the abnormalities caused by irregular glucose levels in blood in the retina of eyes [7]. One of the traits indicating the presence of DR is existence of exudates in the retina [8]. The blood vessels in retina rupture and the lipids that are carried by these vessels tend to accumulate in the posterior pole of fundus image [9]. These accumulations are coined the term Exudates.

Exudates are classified into two categories – hard exudates and soft exudates [10]. Soft exudates are usually harmless. Hard exudates, on the other hand, can cause blurred vision. If they are left untreated or ignored, they can lead to permanent blindness. These abnormalities are noticed in fundus images [11].

This paper deals with implementation of a novel image processing algorithm on an embedded system platform that involves MATLAB and FPGA. MATLAB's Image Processing toolbox is utilized for the same and an Artix 7 FPGA is also employed. The paper is divided into the below mentioned sections. Existing algorithms and proposed work are explained in Section 2 and Section 3 respectively. While Section 4 covers results, Section 5 concludes the paper.

II. EXISTING METHODOLOGIES

The authors in [12] propose application of convolutional neural network (CNN) for exudate classification. The green component is initially tapped out of an RGB image. Since the illumination across a fundus image varies from region to region, an illumination correction algorithm is applied. Looking at the images, it can be clearly noticed that the colour and texture of optic disc (abbreviated as OD) matches with that of exudates. Thus, it becomes a necessity to remove OD first and then extract exudates.

In order to eliminate OD, local phase symmetry algorithm is utilized. In this method, the center of OD is identified and region growing is carried out to engulf the OD, thus eliminating it from the image. In order to remove blood vessels and small dark lesions, morphological opening and closing are employed. Furthermore, candidate points of exudates are analyzed using Ultimate opening. The resulting image is superimposed on modified green image.

This superimposed result is then subtracted from original image to procure precise candidate points of exudates. Later, images are split into templates of size 64 x 64 pixels and are given as input to CNN. Convolutional, maxpooling and fully connected layers of CNN assist in learning these candidate points, so that they can be used for further testing.

According to authors of [13], L* layer of L*u*v* colour model can help in easy exudate extraction. The extracted L* colour model is made to undergo top hat transform. The transformed image is added up with unmodified L* layer. This sum is subtracted from bottom hat transformed image of L* layer, which results in contrast enhanced image. Regional minima are calculated on the contrast adjusted image to further reduce brighter areas of the image. Using regional minima as marker, the preprocessed image is reconstructed based on morphological dilation. The difference between preprocessed image and reconstructed image results in an image where OD and exudates get highlighted and other artifacts get nullified. In order to retain only exudates, OD is removed. This is realized by searching for circular objects in the image. Once the circular object is identified, which indicates OD, its center is located. To mask OD, a circle with its center lying at the coordinates estimated earlier is drawn. The resulting image's maxima are suppressed by implementing H-maxima transform. The exudates are segmented using Renyi Entropy Thresholding, where threshold is calculated by summing up entropies of background and foreground. These entropies are estimated using probability distribution of image.

Ruba and Ramalakshmi [14] propose that the original fundus image must be resized to a resolution of 256 x 256 pixels. To smoothen the image, green channel is extracted, and median filtering is applied. 24 features of the image such as mean, variance and standard deviation at numerous orientations are calculated using Gabor filter. Correlation, entropy, contrast, energy and other 8 features are calculated using Gray level co-occurrence matrix (GLCM). Using these features, a binary support vector machine (SVM) classifier is trained to group the images into two categories – positive and negative. Positive class indicates defective retina and negative class indicates healthy retina. In test mode, if a normal fundus image is fed to the algorithm then the result should be declared as normal and no further processing should be performed on the image. Contrarily, upon feeding an image of defective fundus image, the result should be declared as positive and the defect should also be stated. In case of exudates, OD must be removed using segmentation and morphological operations, thus retaining exudates.

Similar to algorithm explained in [14], authors of [15] suggest that the RGB image has to be reduced in size to 126 x 126 pixels. The resized image must be then converted to a grayscale image. To denoise image, median filter is employed. Next, OD is localized and is segmented using GVK's Snake algorithm. Region growing is utilized to discard non-exudate regions. Later, to perform feature extraction, Gabor filter is deployed.

Jadhav and Patil in [16] insist that the grayscale fundus image has to be filtered using median filtering. In order to attain uniform illumination all over the image, Adaptive Histogram Equalization has to be performed. To extract exudates and OD, segmentation has to be carried out. To extract blood vessels, wavelet transform, matched filter and derivative of Gaussian are employed. To discard OD, windowing method is put to use, according to which the window that consists largest number of white pixels is deemed as the one that contains OD. Mean, variance and standard deviation are calculated for further classification. [17] explains a similar algorithm. In case of [18], matched filtering is used for segmentation.

Ahmed in [19] proposes resizing RGB images to 200 x 280 pixels and extracting green colour layer. Hough transform is applied to eliminate OD. The RGB image is considered again and red and green channels are improvised, without altering blue component. This is done as exudates are clearly visible in red and green channels and not in blue channel. Next, in order to train the algorithm, 500 pixels are chosen, and their pixel intensity values are enlisted. The minimum and maximum points are found out which define the extremes of intensity of exudates 'pixels. All the pixels lying within the extremes are stockpiled into a vector. Average, variance and three times the standard deviation (also known as three-sigma or 3σ) are calculated on this vector. The intensity range for thresholding is defined between standard deviation and three-sigma calculated.

In order to correct illumination of all three channels of RGB, authors of [20] propose to perform shadow correction. For contrast adjustment, median of m x n pixels is calculated and is subtracted from the original pixel values. Red component is picked from RGB image and segmentation based on thresholding is employed to extract OD and exudates. OD is localized using Hough transform and is masked out. In addition to this, RGB image is converted to HSV colour model and local contrast enhancement using local variation and mean is employed. Modified HSV image is converted back to RGB and is then converted to $L\theta\phi$ colour space. R, G, B, L, θ, ϕ together form six-dimensional vector. Different parts of the image are then represented using prototype vectors. Euclidian distance is used to measure distance between vectors and image patterns for template matching. Brightness, colour, shape and other features are considered to identify exudates.

Most of the above-mentioned algorithms use Hough transform and feature extraction, which are not feasible when one thinks about hardware or embedded system-based implementation, as they are computationally complex. Thus, the method explained in next section has been developed carefully such that the steps are not difficult to implement on hardware, thus making the system efficient.

III. PROPOSED SYSTEM

An overview of implementation of the algorithm on hardware and software is showcased in Fig. 1. The first and the foremost task of the designer/developer is to distinguish between the steps that must be implemented on MATLAB and FPGA. To successfully select the implementation procedure, one must acknowledge time consumption,

memory requirement, area efficiency and complexity involved in every step of the proposed algorithm. Considering the above said parameters, image acquisition, colour model selection, OD removal and extraction of exudates are carried out on MATLAB, while average filtering, contrast adjustment, segmentation and morphological operations are performed on FPGA.

The fundus images are collected from DiaRetDB0 [21], DiaRetDB1 [22], IDRiD [23] and MESSIDOR [24] databases.
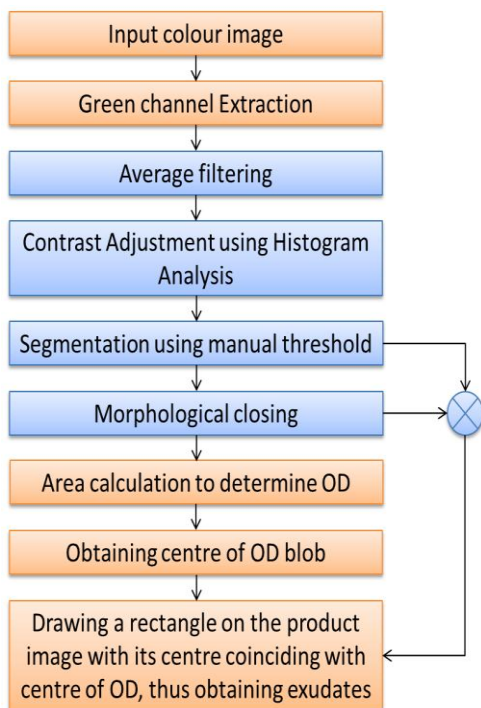

Fig. 1.Flowchart of the algorithm: blocks in blue represent that they have been realized on FPGA, while orange blocks indicate MATLAB implementation

A. Input RGB Image

The fundus image is input in MATLAB. These images are in RGB colour space. Since the resolution of images varies from database to database, all the images are resized to 576 x 720 pixels.

B. Green Channel Extraction

Green channel highlights exudates more than any other colour model or colour layer. Hence it is separated from the input image. This also reduces the computation involved; by selecting one colour plane, one can process only 8 bits per pixel, instead of processing 24 bits if the entire colour model is selected [25]. Fig. 2 shows an RGB fundus image and its extracted green channel.
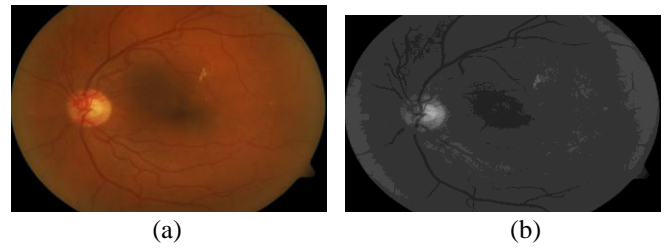

Fig. 2.Fundus image: (a) RGB image (b) Green channel

The pixels of green channel are stored into a coefficient file and passed to FPGA so that they can be stored into a block RAM for further processing. After each step of the algorithm is processed, the results are stored in BRAM, so that the values can be used for the next step.

C. Average filtering

In order to filter out small blemishes and irregularity in pixel intensity distribution, average filtering is performed on the green channel image. The entire image is divided into 3x3 image patches for calculating mean of pixels. The mean of all 9 pixels corresponding to a patch is calculated and these pixels are replaced by the resulting average [26].

For an image patch of 3x3 pixels, whose intensity values are represented as x_0, x_1, x_2, x_3, x_4, x_5, x_6, x_7, and x_8, the mean (μ) is calculated as shown in (1).

$$\mu = \frac{x_0 + x_1 + x_2 + x_3 + ... + x_9}{9} \qquad (1)$$

To calculate mean, the sum of 9-pixel values is divided by 9 using the method of restoring division [27]. The flowchart of division algorithm is shown in Fig. 3. Fig. 4 shows the mean filtered image output.
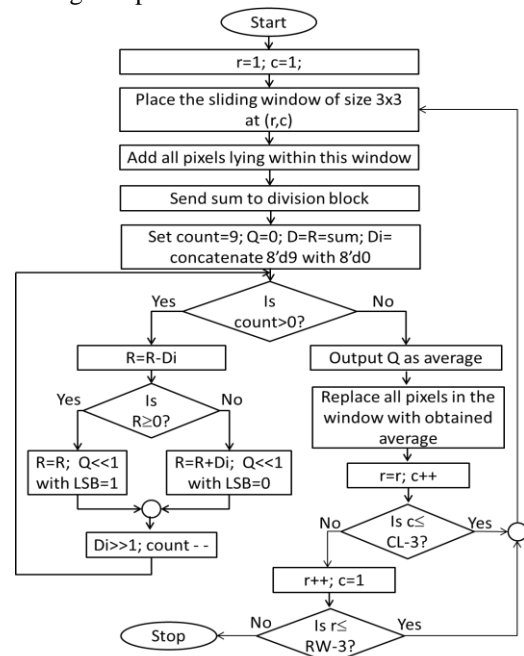

Fig. 3.Average filtering flowchart with restoring division; r is index of row, c is index of column, RW is total number of rows, CL is total number of columns in the image, Q is quotient, count represents number of iterations, Di is divisor

D. Contrast Adjustment

In order to gain uniformity in contrast across the image, contrast enhancement is performed. Thus, histogram-based contrast enhancement method is applied. The plot of frequency of pixels (also known as counts) against intensity of pixels (also referred as bins) is called Histogram [28]. The histogram obtained over the average filtered image is shown in Fig. 5. Fig. 6 shows the workflow to be followed to obtain histogram on FPGA.
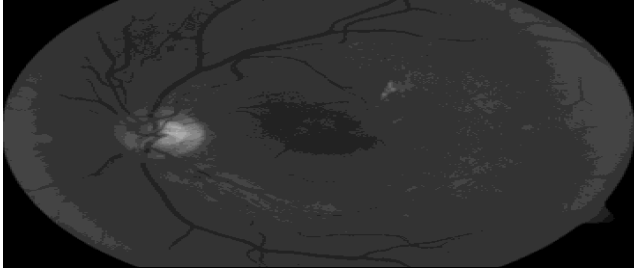

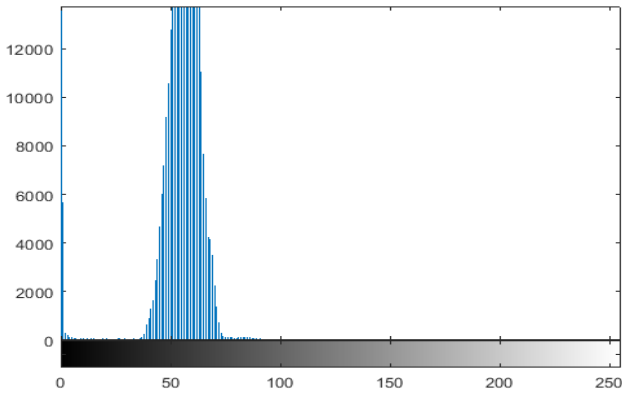**Fig. 4.Image obtained after performing Average filtering over the extracted green channel.**

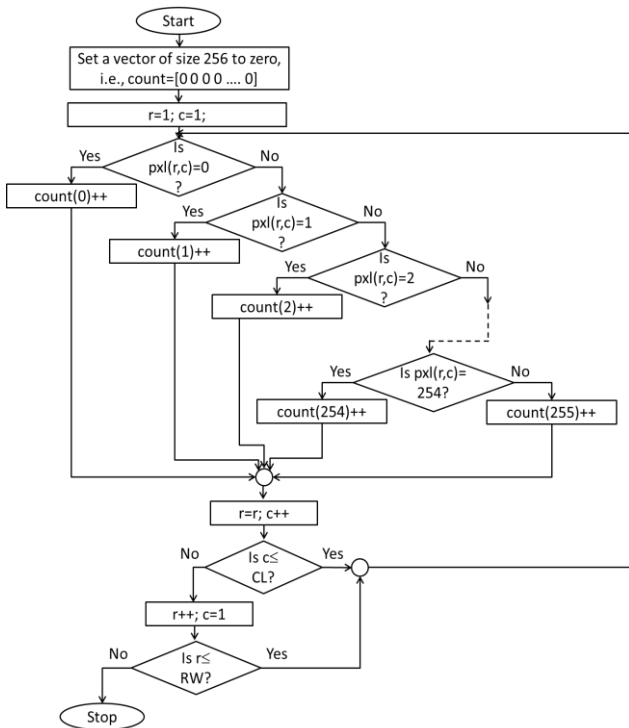**Fig. 5.Histogram of image obtained after average filtering**

Fig. 6.Histogram flowchart; r is index of row, c is index of column, RW is total number of rows, CL is total number of columns in the image

Let pixel values be $bins = \{0, 1, 2, \ldots., 254, 255\}$ and the corresponding counts be $counts = \{count_0, count_1, count_2, \ldots., count_{254}, count_{255}\}$. The pixel counts whose frequencies are more than 100 are added up, and the sum is represented as N, as shown in (2).
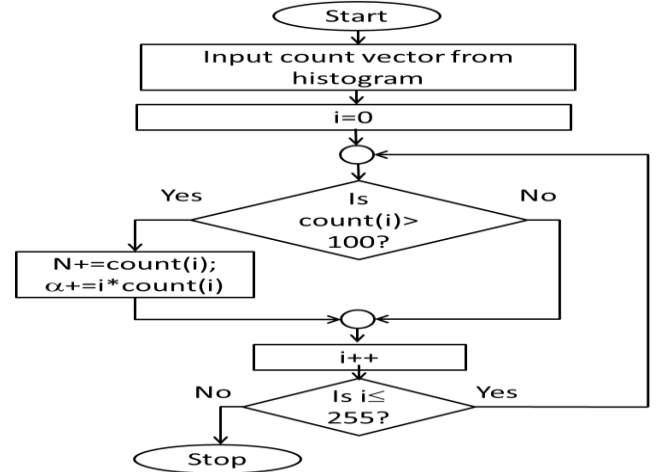
$$N = \sum_{0}^{255} counts(i); \forall counts(i) > 100 \qquad (2)$$

Also, the counts considered in (2) are multiplied with their respective pixel intensity values, and these products are summed up, as shown in (3). The sum obtained is represented as α. Fig. 7a depicts this process in a flowchart.

$$\alpha = \sum_{0}^{255} bins(i) * counts(i); \forall counts(i) > 100 \qquad (3)$$

Sum of products (α) is then divided by sum of counts (N) to obtain a value, symbolized as δ, which serves as the mean of the pixels whose counts are greater than 100. This can be represented as shown in (4) and by Fig. 7b. Division is performed using unsigned binary division [29].

$$\delta = \frac{\alpha}{N} \qquad (4)$$

(a)

(b)

Fig. 7.Flowcharts depicting (a) Obtaining α and N, and (b) Calculating δ from α and N using unsigned binary division

To enhance the contrast of the areas which imbibe exudates and OD, pixels of average filtered image are compared with δ. If pixel intensity is greater than δ, then it is multiplied with 2, otherwise it is divided by 2. In a hardware perspective, product resulting from multiplying a pixel value with 2 can be obtained by applying left shift by one position operation on the value. Similarly, logically shifting a pixel value to right by one position equates to division of the pixel value by 2. This is expressed using (5). The resulting image is showcased in Fig. 8.

$$ca_{(x,y)} = \begin{cases} avg_{(x,y)} >> 1 & , avg_{(x,y)} \geq \delta \\ avg_{(x,y)} << 1 & , avg_{(x,y)} < \delta \end{cases} \quad (5)$$
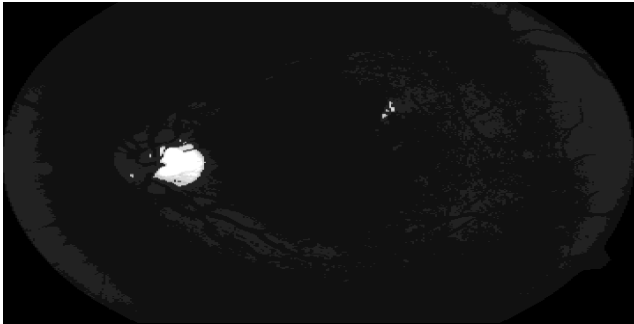

Fig. 8.Image resulting from contrast enhancement.

E. Segmentation

Due to contrast enhancement, the pixels corresponding to exudates get brighter and are found to be of higher contrast compared to background. Thus, simple thresholding is performed to obtain binary image. A threshold of 135 is set. All pixels with intensity greater than or equal to the threshold are converted to white, represented by '1', while the pixels with intensities less than 135 are converted to black, depicted by '0' [30], as depicted in (6). This leads to extraction of both exudates and OD, as their colour and texture are almost similar. This process is showcased in Fig. 9. Fig .10 shows the resulting binary image.

$$seg_{(x,y)} = \begin{cases} 1, & ca_{(x,y)} \geq 135 \\ 0, & otherwise \end{cases} \quad (6)$$
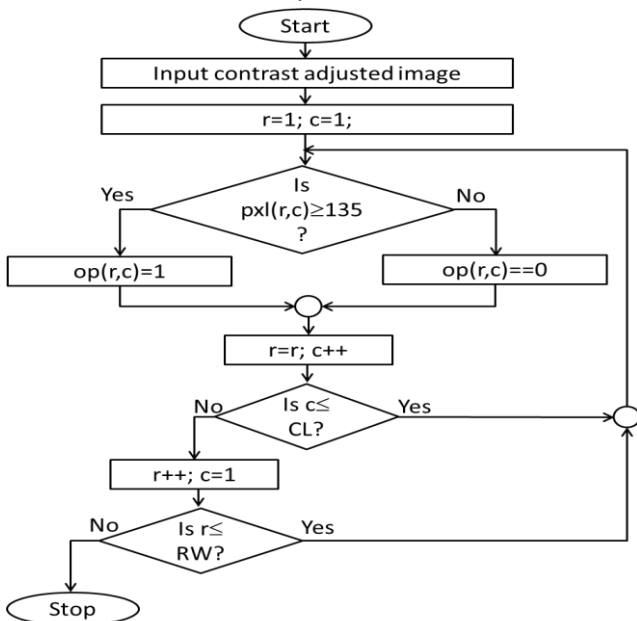

Fig. 9.Thresholding flowchart

Fig. 10. Image resulting from thresholding operation.

F. Morphological Closing

Since the pixel values of OD and exudates match, segmentation on the contrast adjusted image often results in both extraction of both OD and exudates. Blood vessels run through OD. The pixels belonging to these vessels often have lower intensity than those lying in the area of OD. This makes blood vessels' area black upon segmentation and OD area to white. This causes OD to disintegrate. The first task is to make sure that all the blobs belonging to OD accumulate to form one huge white blob. To attain this objective, morphological dilation is performed. A structuring element of shape 'disk' and radius 7 is chosen.

Structuring element is a reference matrix/window that moves across the image. The pixel that lies to the centre of this reference matrix is considered as "centre pixel", while the surrounding pixels are named as "neighbouring pixels". Structuring element of shape disk with radius of 7 pixels closely approximates to a square matrix of size 13x13 pixels, where pixels at co-ordinates (0,0), (0,1), (0,11), (0,12), (1,0), (1,12), (11,0), (11,12), (12,0), (12,1), (12,11) and (12,12) are ignored, thus creating an illusion of a "disk" shaped matrix. The pixel lying at coordinate (6,6) is considered as the centre pixel. As per the definition of binary dilation [31], if any of the neighboring pixels is white, then the center pixel is made white, irrespective of its previous state. In case of absence of a white pixel in the neighborhood, the center pixel is retained as it is. The flowchart in Fig. 11 depicts how dilation is implemented on FPGA, where r is index of row, c is index of column, RW is total number of rows, CL is total number of columns in the image.

Further, to eliminate the spare pixels neither belonging to exudates nor OD, morphological erosion is conducted. Erosion is the complement of dilation; the center pixel is changed to black if at least one black pixel is found in its neighborhood. The chosen structuring element is same as that employed for dilation. The process in which erosion is carried out on a dilated image with same structuring element is known as Morphological closing [32]. The flowchart in Fig. 12 depicts how erosion is implemented on FPGA. The image resulting from closing is shown in Fig. 13.

Sometimes, due to application of morphological closing, the blobs tend to outgrow their original size. This implies that morphological operations may tamper the area of exudates.

In order to overcome this increase in number of pixels of exudates, closed image is multiplied with segmented image, thus eliminating noisy pixels and outgrown pixels.

Fig. 11.   Dilation flowchart

Fig. 12.   Erosion flowchart

Fig. 13.   Image resulting from morphological closing.

Once these processes are complete on FPGA, two .dat files are created – one to store all the pixel intensities corresponding to closed image, and the other to store the pixels obtained after multiplying closed image with segmented image. These two .dat files are read in MATLAB and the rest of the steps involved in the algorithm are carried out.

G. Removal of OD

It is well established fact that the size of OD is always larger than individual blobs of exudates [33]. Connected component labelling is carried out on the closed image obtained from FPGA to estimate area of every white blob [34]. Each connected component is tagged with a number or a 'label'. The frequency of each label indicates the area or number of pixels corresponding to that label. The label with highest frequency is deemed as OD. The other blobs are replaced with black pixels, thus retaining only OD. The centre of OD is calculated using 'regionprops' command of MATLAB [35]. The image obtained after retaining only OD is shown in Fig. 14.

Fig. 14.   OD extracted; the red dot on OD indicates its centre.

It was found out from the dataset considered that the maximum diameter of the OD is found to be 200 pixels. Thus, in order to extract exudates a zero matrix of size 200x200 pixels is drawn on the image obtained after multiplication, with its center coinciding with the center of OD detected. Fig. 15 shows the final image obtained after the complete processing is done.
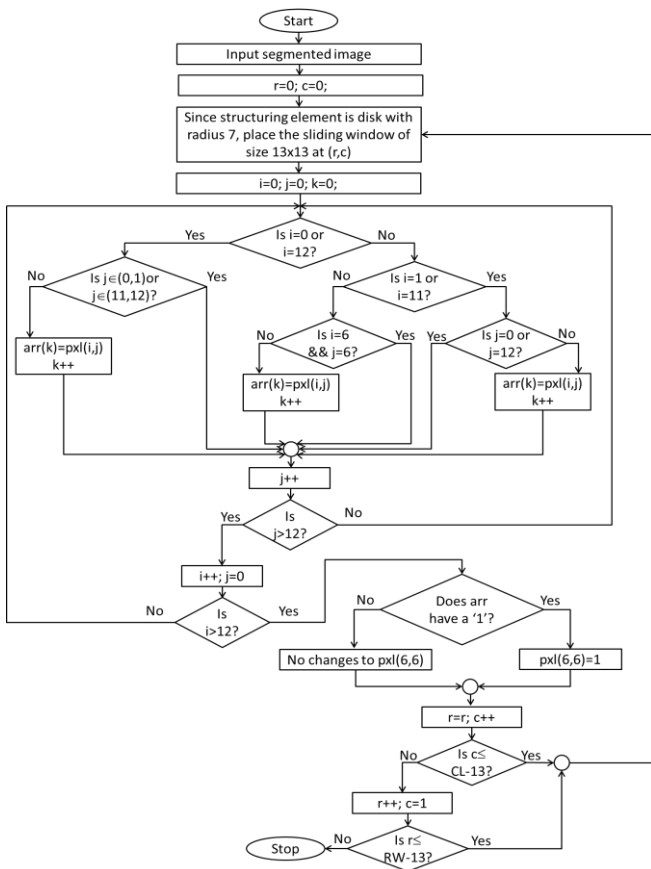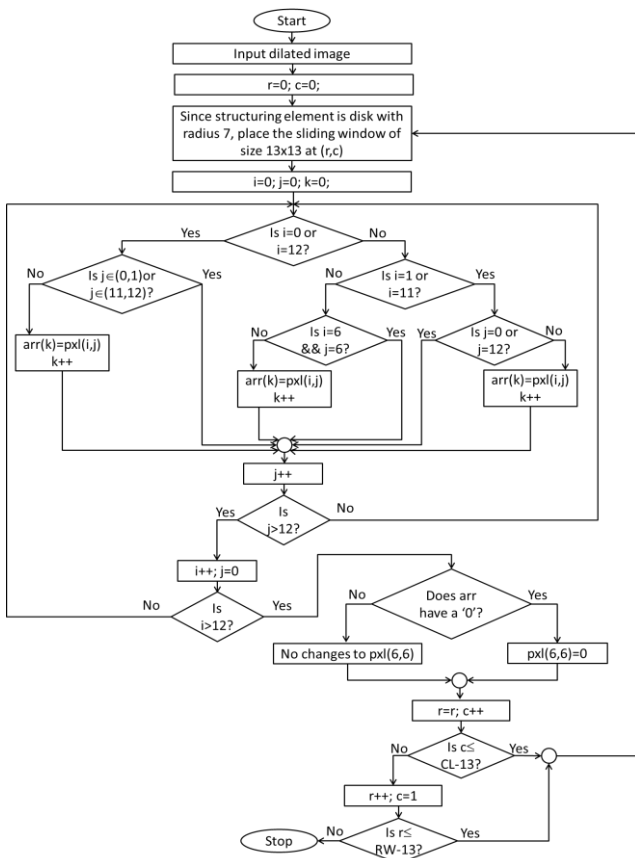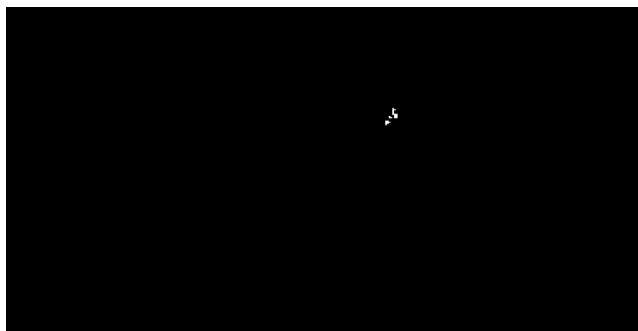
Fig. 15. Exudates extracted

IV. RESULTS

The algorithm has been tested for 60 images. 51 images yielded accurate outputs, successfully detecting all exudates. 3 images which do not have exudates were also fed as inputs, which again were correctly diagnosed. 4 images are also loaded to this algorithm, in which few exudates were lost due to their extremely small size or due to their close proximity to OD, which are eliminated due to the square drawn. In 2 cases, blood vessels were wrongly diagnosed as exudates. To validate the results, true positive (TP), true negative (TN), false positive (FP) and false negative (FN) were calculated. Using these values, accuracy was calculated using (7) [36] and was found to be 90%.

$$Accuracy = \frac{TP + TN}{TP + TN + FP + FN} \quad (7)$$

The synthesis results for the steps implemented on Artix 7 (XC7A100TCSG324-2) FPGA [37] with a timing constraint of 10 nanoseconds are disclosed in Table I. The values were synthesized using Vivado 2017.2.

Table- I: Synthesis Summary on XC7A100TCSG324-2

Circuits realized using Verilog for FPGA	Time Delay (nanoseconds)	Area (%)
Average filtering	8.011	0.24
Contrast Adjustment	13.417	7.08
Segmentation	1.894	<0.01
Dilation	3.857	0.12
Erosion	3.857	0.12
Image multiplication	0.991	<0.01

Also, the synthesis values obtained for restoring division and unsigned binary division are shown below in Table II.

Table-II: Division Synthesis Summary

Division Circuits	Time Delay (nanoseconds)	Area (%)
Restoring Division	2.795	0.09
Unsigned binary division	5.3	0.55

V. CONCLUSION

As explained in [38], embedded systems are faster than the traditional software approach for biomedical applications of image processing. In this paper, a novel method for extraction of exudates and elimination of OD using MATLAB and FPGA is explained. The proposed method uses statistical analysis on histogram to improve the constrast of fundus images. Manual thresholding, Morphological operations and connected component labelling are employed to extract exudates. The steps are carefully chosen for hardware and software implementation. An accuracy of 90% is acquired using this technique. As future scope, the software part can be implemented on Python using OpenCV, to make the system further cost-effective.

REFERENCES

1. Ming-Chien Chyu, Tony Austin, Fethi Calisir, Samuel Chanjaplammootil, Mark J. Davis, Jesus Favela, Heng Gan, Amit Gefen, Ram Haddas, Shoshana Hahn-Goldberg, Roberto Hornero, Yu-Li Huang, Øystein Jensen, Zhongwei Jiang, J.S. Katsanis, Jeong-A Lee, Gladius Lewis, Nigel H. Lovell, Heinz-Theo Luebbers, George G. Morales, Timothy Matis, Judith T. Matthews, Lukasz Mazur, E.Y.K. Ng, K.J. Oommen, Kevin Ormand, Tarald Rohde, Daniel Sánchez-Morillo, Justo García Sanz-Calcedo, Mohamad Sawan, Chwan-Li Shen, Jiann-Shing Shieh, Chao-Ton Su, Lilly Sun, Mingui Sun, Yi Sun, Senay N. Tewolde, Eric A. Williams, Chongjun Yan, Jiajie Zhang, Yuan-Ting Zhang. "Healthcare Engineering Defined – a White Paper", Journal of Healthcare Engineering, Vol. 6, No. 4, Page 635–648, 2015.
2. Jain, Sanjeev & G. Patil, Bhagyashri. (2014). Cancer Cells Detection Using Digital Image Processing Methods. International Journal of Latest Research in Science and Technology. VOLUME 3. 45-49.
3. S. R. Telrandhe, A. Pimpalkar and A. Kendhe, "Detection of brain tumor from MRI images by using segmentation & SVM," 2016 World Conference on Futuristic Trends in Research and Innovation for Social Welfare (Startup Conclave), Coimbatore, 2016, pp. 1-6.
4. A. Ajith, V. Goel, P. Vazirani and M. M. Roja, "Digital dermatology: Skin disease detection model using image processing," 2017 International Conference on Intelligent Computing and Control Systems (ICICCS), Madurai, 2017, pp. 168-173.
5. Satyananda V., Narayanaswamy K.V., Karibasappa (2020) An Embedded System for Watershed Based Hard Exudate Extraction. In: Abraham A., Cherukuri A., Melin P., Gandhi N. (eds) Intelligent Systems Design and Applications. ISDA 2018 2018. Advances in Intelligent Systems and Computing, vol 940. Springer, Cham
6. Shouip, Hossam. (2014). Diabetes mellitus.
7. Boyd, K., "What is Diabetic Retinopathy", American Academy of Ophthalmology, Sept 01, 2017. Available Online: https://www.aao.org/eye-health /diseases/what-is-diabetic-retinopathy
8. Elia Duh, "Non-proliferative Diabetic Retionopathy" in Diabetic Retinopathy, Humana Press, Baltimore, USA, pp 4.
9. M.Ramaswamy , D.Anitha, S.Priya Kuppamal, R.Sudha, S.Fepslin Athish Mon, A Study and comparison of automated technique for exudate detection using digital fundus image of human eye: A review for early identification of Diabetic Retinopathy, Int.J. Comp. Tech. Appl. 2(5)(2011)1503-1516
10. Esmann V, Lundbaek K, Madsen PH. Types of exudates in diabetic retinopathy. Acta Med Scand. 1963;174:375–84.
11. Satyananda, Vasanthi & Narayanaswamy, K.V & Karibasappa. (2019). Hard Exudate Extraction from Fundus Images using Watershed Transform. Indonesian Journal of Electrical Engineering and Informatics (IJEEI). Vol. 7, No. 3, Sep 2019, pp. 449~462
12. S. Yu, D. Xiao and Y. Kanagasingam, "Exudate detection for diabetic retinopathy with convolutional neural networks," 2017 39th Annual International Conference of the IEEE Engineering in Medicine and Biology Society (EMBC), Seogwipo, 2017, pp. 1744-1747.
13. D. U. N. Qomariah and H. Tjandrasa, "Exudate detection in retinal fundus images using combination of mathematical morphology and Renyi entropy thresholding," 2017 11th International Conference on Information & Communication Technology and System (ICTS), Surabaya, 2017, pp. 31-36.
14. T. Ruba and K. Ramalakshmi, "Identification and segmentation of exudates using SVM classifier," 2015 International Conference on Innovations in Information, Embedded and Communication Systems (ICIIECS), Coimbatore, 2015, pp. 1-6.

15. P. Patil, P. Shettar, P. Narayankar and M. Patil, "An efficient method of detecting exudates in diabetic retinopathy: Using texture edge features," 2016 International Conference on Advances in Computing, Communications and Informatics (ICACCI), Jaipur, 2016, pp. 1188-1191.
16. A. S. Jadhav and P. B. Patil, "Detection of exudates for diabetic retinopathy using wavelet transform," 2017 IEEE International Conference on Power, Control, Signals and Instrumentation Engineering (ICPCSI), Chennai, 2017, pp. 568-571.
17. P. Kokare, "Wavelet based automatic exudates detection in diabetic retinopathy," 2017 International Conference on Wireless Communications, Signal Processing and Networking (WiSPNET), Chennai, 2017, pp. 1022-1025.
18. H. A. Nugroho, K. Z. W. Oktoeberza, I. Ardiyanto, R. L. B. Buana and M. B. Sasongko, "Automated segmentation of hard exudates based on matched filtering," 2016 International Seminar on Sensors, Instrumentation, Measurement and Metrology (ISSIMM), Malang, 2016, pp. 84-87.
19. M. S. Ahmed and B. Indira, "Detection of exudates from RGB fundus images using 3σ control method," 2017 International Conference on Wireless Communications, Signal Processing and Networking (WiSPNET), Chennai, 2017, pp. 767-770.
20. A. C. Somkuwar, T. G. Patil, S. S. Patankar and J. V. Kulkarni, "Intensity features based classification of hard exudates in retinal images," 2015 Annual IEEE India Conference (INDICON), New Delhi, 2015, pp. 1-5.
21. Kauppi, T., Kalesnykiene, V., Kamarainen, J.-K., Lensu, L., Sorri, I., Uusitalo, H., Kälviäinen, H., Pietilä, J., DIARETDB0: Evaluation Database and Methodology for Diabetic Retinopathy Algorithms, Technical report
22. Kauppi, T., Kalesnykiene, V., Kamarainen, J.-K., Lensu, L., Sorri, I., Raninen A., Voutilainen R., Uusitalo, H., Kälviäinen, H., Pietilä, J., DIARETDB1 diabetic retinopathy database and evaluation protocol, Technical report
23. Porwal, P.; Pachade, S.; Kamble, R.; Kokare, M.; Deshmukh, G.; Sahasrabuddhe, V.; Meriaudeau, F., Indian Diabetic Retinopathy Image Dataset (IDRiD): A Database for Diabetic Retinopathy Screening Research. Data 2018, 3, 25.
24. Decencière et al.. Feedback on a publicly distributed database: the Messidor database, Image Analysis & Stereology, v. 33, n. 3, p. 231-234, aug. 2014. ISSN 1854-5165.
25. S. R. Rupanagudi, S. Huddar, V. G. Bhat, S. S. Patil and Bhaskar M. K., "Novel methodology for Kannada Braille to speech translation using image processing on FPGA," 2014 International Conference on Advances in Electrical Engineering (ICAEE), Vellore, 2014, pp. 1-6.
26. M. Ghosh and S. Mukhopadhyaya, "Cache oblivious algorithm of average filtering in image processing," 2012 International Conference on Informatics, Electronics & Vision (ICIEV), Dhaka, 2012, pp. 149-154
27. Kumar, D., Saha, P., Dandapat, A.: Hardware implementation of methodologies of fixed-point division algorithms. Int. J. Smart Sens. Intell. Syst. 10, 630–645 (2017).
28. Komal, Vij & Yaduvir, Singh. (2011). Enhancement of Images using Histogram Processing Techniques. International Journal of Computer Technology and Applications.
29. T. A. Moniem, All Optical Binary Divider, International journal of optics and applications, PP 22-26, Jan 2012.
30. S. R. Rupanagudi et al., "A simplified approach to assist motor neuron disease patients to communicate through video oculography," 2018 International Conference on Communication information and Computing Technology (ICCICT), Mumbai, 2018, pp. 1-6.
31. S. R. Rupanagudi et al., "A novel and secure methodology for keyless ignition and controlling an automobile using air gestures," 2016 International Conference on Advances in Computing, Communications and Informatics (ICACCI), Jaipur, 2016, pp. 1416-1422.
32. H. Hamid, S. Najmeh, S.M.M. Salehi, Using morphological transforms to enhance the contrast of medical images, Egypt. J. Radiol. Nucl. Med., 46 (2015) 481-489.
33. "The COMS Grading Scheme: Graded Features", Carver College of Medicine, The University of Iowa, 2006. Available Online: http://webeye.ophth.uiowa.edu/
34. He, L., X. Ren, Q. Gao, X. Zhao, B. Yao, and Y. Chao. "The Connected-Component Labeling Problem: A Review of State-of-the-Art Algorithms." Pattern Recognition, 70:25--43, 2017
35. In.mathworks.com. (2018). Measure properties of image regions - MATLAB regionprops- MathWorks India. [online] Available at: https://in.mathworks.com/help/images/ref/regionprops.html [Accessed 14 Sep. 2018].
36. Vijay Kotu, Bala Deshpande, Chapter 8 - Model Evaluation, Editor(s): Vijay Kotu, Bala Deshpande, Data Science (Second Edition), Morgan Kaufmann, 2019, Pages 263-279, ISBN 9780128147610, https://doi.org/10.1016/B978-0-12-814761-0.00008-3.
37. 7 Series FPGAs - Configurable Logic Block, UG474 (v1.8) September 27, 2016.
38. V. Satyananda, K. V. Narayanaswamy and Karibasappa, "An embedded system based solution for exudate extraction," 2017 International Conference on Robotics, Automation and Sciences (ICORAS), Melaka, 2017, pp. 1-5

AUTHORS PROFILE

Prof. Vasanthi Satyananda, who is currently an Associate Professor at Atria Institute of Technology, Bangalore, India and an alumnus of UVCE, Bangalore, has obtained her Bachelor of Engineering degree in Electronics and Communication engineering from Bangalore University. She has completed her Master's degree in Electronics Engineering at BMSCE, affiliated to Bangalore University. Presently she is pursuing her doctoral degree in the field of Image Processing and VLSI in VTU. She also has obtained post diploma certificate in Digital Communication from LRDE, Bengaluru. She has a combined experience of thirty years, twelve years of which have been in industries. She began her career in Bharath Electronics Limited, Bengaluru. After a year of service with BEL, she joined Karnataka Telecom Limited, Bengaluru and served for eight more years. She completed her career in industries after serving for three more years in International Instruments Limited, Bengaluru. She started her teaching career in the year 2000 and worked various capacities like HoD for departments of Telecommunication and Electronics and Communication, Dean Academics etc. She has authored 14 research articles till date for reputed papers and journals indexed by IEEE, Elsevier Scopus and Springer and several other papers for different international journals and national conferences.

Dr. K. V. Narayanaswamy, who is currently the Principal at Atria Institute of Technology, Bangalore, India, received his Ph.D degree in Electrical & Electronics Engineering, specialised in Wireless & Mobile Ad-Hoc networks from Visvesvaraya Technological University, Belgaum, Karnataka. He has more than 26 years of teaching & research experience in the field of Electrical, Electronics & Communication Engineering. Worked in several prestigious institutions including PES Institute of Technology, M.S. Ramaiah University of Applied Sciences, visited several countries under various schemes including Coventry University UK, under UKIERI (UK-INDIA Education and Research Initiatives), Bahrain, United Arab Emirates. Research interests are in the areas of next-generation wireless communications, Mobile Ad-hoc & wireless sensor networks, advanced optical network design, automotive communication protocols and standards. He has also carried several research, consultancy and funded projects. He has delivered number of corporate trainings both in India and abroad including for Tata Motors, Satyam Mahindra, Mahindra Research Valley, WIPRO etc. He has published more than 16 papers in peer reviewed international journals like IEEE, IJCA, IJCET, IJSRPB, Elixir etc., and several conference papers.

Dr. K Karibasappa, who is currently a Professor at Dept. of ECE, Dayananda Sagar Academy of Technology & Management, Kanakapura Main Road, Bengaluru, India, completed his Ph.D in Machine Learning and Perception Using Cognitive Method from University College of Engineering, Burla, Orissa Sambalpur University in 2004. He did his Master of Engineering on Electronics and Telecommunication from Jadavpur University, 1998, Calcutta, West Bengal and Bachelor of Engineering on Electronics and Communication from Malnad College of Engineering. He has thirty-two years of service in academics. He has held various positions like Principal, Vice Principal, Dean, Professor etc. He has fifty plus research papers to his credit. His area of interest are Machine Learning and Artificial Intelligence.